

# Fracture-energy scaling in dynamic models of past Earthquakes as a constraint for physics-based ground-Motion simulations

**M. Causse**

*ISTerre, Université Grenoble-I, IFSTTAR, France*

**L. Dalguer**

*ETH Zürich, Switzerland*

**P.M Mai**

*King Abdullah University of Science and Technology, Saudi Arabia*



## SUMMARY:

We analyze the scaling of average dynamic source properties (fracture energy, static stress drop and dynamic stress drop) from a suite of 33 kinematic inversion models from 22 crustal earthquakes. Shear-stress histories are first computed solving the elastodynamic equations by imposing slip velocity, obtained from kinematic inversion, as a boundary condition on the fault plane. This is achieved by means of a 3D finite difference method in which the rupture kinematics are modeled with the Staggered-Grid-Split-Node (SGSN) fault representation method of Dalguer and Day (2007). Dynamic parameters are then estimated from the calculated stress-slip curves and averaged over the fault plane.

We show that fracture energy is highly sensitive to average rise-time and to the roughness degree of static slip. An uncertainty analysis reveals that despite the poor resolution of kinematic inversion models, our dynamic parameter estimations are rather stable. Our results indicate that fracture energy and stress drop increase with magnitude. Given the sensitivity of fracture energy to slip roughness, we propose new scaling relations (fracture energy vs. seismic moment and slip roughness) that may be useful to constrain the initial conditions in spontaneous dynamic rupture calculations for earthquake source studies and physics-based near-source ground-motion prediction for seismic hazard and risk mitigation.

*Keywords: Earthquake source scaling, Fracture energy, Kinematic source model*

## 1. INTRODUCTION

The earthquake rupture process distributes accumulated strain energy into fracture energy, radiated seismic energy and heat. In this context, the term “fracture energy” comprises any energy loss phenomena involved in the rupture expansion, and thus needs to be distinguished from the “surface fracture energy” of linear elastic fracture (Cocco and Tinti, 2008). Quantifying the energy balance for the dynamic rupture process remains not only a crucial issue in earthquake seismology, but also for ground-motion estimation and seismic hazard because rupture dynamics control the radiated seismic energy.

Current efforts in advanced source modelling aim to integrate basic principles of rupture mechanics, through so-called “pseudo-dynamic” models (which are kinematic models that include the main features of earthquake source dynamics, *e.g.* Guatteri et al. 2004) or fully dynamic spontaneous rupture simulations. Given the increasing high-performance computation resources, dynamic simulation are considered to be routinely used for near-source ground-motion prediction. However, they require a full description of the friction law that governs the slip weakening process on the fault

plane (static and dynamic stress drop, slip weakening distance), which in itself remains poorly understood as many (partially competing) processes at the crack tip of the expanding rupture front interact with each other (*e.g.* Bizzarri, 2010).

Many studies have been carried out to characterize the slip weakening behavior from the source kinematics. The principle is to retrieve the stress history on each point of the fault plane as dictated by the slip history obtained from kinematic inversion (*e.g.* Fukuyama et al. 2003, Mikumo et al. 2003). For instance, these authors show evidence of a correlation between the time of maximum slip velocity and the breakdown time (time of minimum shear stress). It is important to note that small scale features of the rupture process cannot be resolved because the kinematic inversions are generally performed at low-frequency (<1 Hz) (Spudich and Guatteri 2004) and require arbitrary choices like the fixed shape of the source-velocity function (Tinti et al. 2009, Piatanesi et al. 2004). Besides, it has been clearly shown that in the current state of knowledge kinematic inversion techniques only provide a gross description of the “true” rupture history (*e.g.* Mai et al. 2007), the details being often just artifacts. This is due to the inherent non-uniqueness of the inverse problem, errors in the forward model parameterization and user-dependent *a priori* choices in the inversion process (*e.g.* inversion method, smoothing constraints, data selection).

The goal of this paper is not to study the details of the earthquake source dynamics. Instead, we aim to constrain several average, global dynamic source features and examine their potential scaling properties (with seismic moment). In particular, we focus on fracture energy. We assess the average fracture energy from a set of past earthquakes for which finite-source rupture models are available. We carried out several test to check if poorly resolved kinematic inversion models can still carry useful information on the scaling of dynamic source properties. We took advantage of a large source model database (<http://www.seismo.ethz.ch/static/srcmod/>) and analyzed a suite of 33 rupture models from 23 events with  $M_w$  ranging from 5.5 to 7.7. We finally proposed different empirical models for fracture energy that can be used in advanced source modeling for ground-motion simulation such as “pseudo-dynamic” models or spontaneous rupture simulations.

## 2. METHOD

Our global strategy is to constrain average fracture energy from a set of earthquakes for which reliable finite-source rupture models are available. The principle is first to retrieve the spatio-temporal shear stress distribution from the source kinematics to constrain the distribution of dynamic parameters on the fault plane. Those parameters are then averaged over the slipping area, and analyzed with respect to their scaling properties

Shear-stress histories are locally computed using the elastodynamic equations of motion using the slip velocity distribution from kinematic inversion as a boundary condition on the fault plane (Figure 2.1). This is achieved by means of a 3D finite difference method. The numerical code is based on the traction-at-split-node method adapted to the velocity-stress staggered-grid finite difference scheme (Dalguer and Day, 2007). The code, initially developed for spontaneous dynamic rupture simulations, has been adapted to be suitable for such kinematically constrained calculations.

Our proxy for fracture energy is the breakdown work ( $W_b$ ) defined by Tinti et al. (2005a):

$$W_b = \int_0^{\tau_b} (\tau(t) - \tau_{\min}) \cdot \dot{u}(t) dt \quad (2.1)$$

where  $\tau(t)$  is the shear stress history,  $\dot{u}(t)$  is slip velocity and  $T_b$  is the time corresponding to the minimum traction  $\tau_{min}$ . The quantity  $W_b$  represents the energy density expended to allow the rupture to propagate. As such, it includes several processes occurring at the expanding crack tip such as surface energy and off-fault plasticity, but also energy loss due to heat. It thus differs from the classical definition of fracture energy in mechanics (see discussion in Cocco and Tinti, 2008).

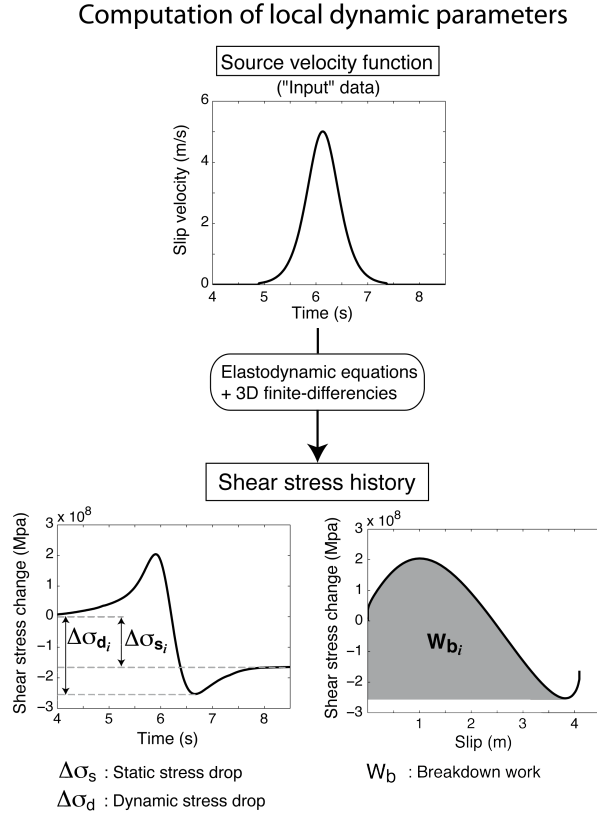


**Figure 2.1.** Sketch for computing the breakdown work (our proxy for fracture energy) at a given point  $i$  of the fault plane, from the source velocity functions obtained from kinematic inversion. The breakdown work corresponds to the shaded area. The displayed curves are for the model by Semmane et al. (2005b) for the 2000 Tottori earthquake, at the maximum slip zone.

### 3. DATA AND DATA PREPARATION

To analyze the scaling of the average fracture energy, we use a dataset of 33 kinematic source inversion models from 23 crustal earthquakes (Table 3.1). Since such rupture models are usually obtained on coarse grids (grid spacing  $\sim 1$ -10 km), they need to be interpolated to ensure stability in the 3D-numercial calculations and to accurately retrieve the shear-stress history. We chose various grid interpolations, ranging from 50 m (for small events, having short rise time and thus needing a good spatial resolution) to 300 m (for the largest events), and adopted a cubic interpolation. However, interpolation tends to decrease the average slip (at areas where the 2<sup>nd</sup> spatial derivative of slip is large). Consequently, as proposed by Tinti et al. (2005a), we follow an iterative procedure to scale the raw slip distribution until the interpolated slip averaged on a given subfault reaches the initial slip value. This results in slightly higher dynamic parameter values.

**Table 3.1.** Selected source inversion models. Events and source models were selected in the database of finite-source rupture models (<http://www.seismo.ethz.ch/static/srcmod>), except for Miyagi-Iwate Nairiku.

| <b>Evt</b> | <b>Location</b>        | <b>Date</b> | <b>Mw</b> | <b>Reference</b>            |
|------------|------------------------|-------------|-----------|-----------------------------|
| 1          | Iwate-Miyagi Nairiku   | 06/14/2008  | 6.9       | Suzuki et al. (2010)        |
| 2          | Fukuoka                | 03/20/2005  | 6.7       | Asano et al. (2006)         |
| 3          | Parkfield              | 09/28/2004  | 6.0       | Custodio et al. (2005)      |
| 4          | Boumerdes              | 05/21/2003  | 7.2       | Semmane et al. (2005a)      |
| 5          | Tottori                | 10/06/2000  | 6.7       | Semmane et al. (2005b)      |
| 6          | Tottori                | -           | -         | Iwata and Sekiguchi (2002)  |
| 7          | Izmit                  | 08/17/1999  | 7.6       | Delouis et al. (2002)       |
| 8          | ChiChi                 | 09/20/1999  | 7.6       | Sekiguchi et al. (2000)     |
| 9          | ChiChi                 | -           | -         | Ma et al. (2001)            |
| 10         | ChiChi                 | -           | -         | Chi et al. (2001)           |
| 11         | Yamaguchi              | 06/25/1997  | 5.8       | Miyakoshi et al. (2000)     |
| 12         | Kagoshima              | 03/26/1997  | 6.0       | Miyakoshi et al. (2000)     |
| 13         | Kagoshimaen-hobu-seibu | 05/13/1997  | 6.1       | Hirokawa (2001)             |
| 14         | Colfiorito 1           | 09/26/1997  | 5.7       | Hernandez et al. (2004)     |
| 15         | Colfiorito 2           | 09/26/1997  | 6.0       | Hernandez et al. (2004)     |
| 16         | Colfiorito 3           | 10/14/1997  | 5.9       | Hernandez et al. (2004)     |
| 17         | Kobe                   | 01/17/1995  | 6.9       | Wald (1996)                 |
| 18         | Kobe                   | -           | -         | Yoshida et al. (1996)       |
| 19         | Northridge             | 01/17/1994  | 6.8       | Wald et al. (1996)          |
| 20         | Northridge             | -           | -         | Hartzell et al. (1996)      |
| 21         | Northridge             | -           | -         | Dreger (1995)               |
| 22         | Landers                | 06/28/1992  | 7.2       | Wald and Heaton (1994)      |
| 23         | Landers                | -           | -         | Hernandez et al. (1999)     |
| 24         | Landers                | -           | -         | Cotton and Campillo (1995)  |
| 25         | Loma Prieta            | 10/18/1989  | 6.9       | Wald et al. (1991)          |
| 26         | Saguenay               | 11/25/1988  | 5.8       | Hartzell et al. (1994)      |
| 27         | North Palm Springs     | 07/08/1986  | 6.1       | Mendoza and Hartzell (1988) |
| 28         | North Palm Springs     | -           | -         | Hartzell (1989)             |
| 29         | Borah Peak             | 10/28/1983  | 6.8       | Mendoza and Hartzell (1988) |
| 30         | New Brunswick          | 01/09/1982  | 5.5       | Hartzell et al. (1994)      |
| 31         | Imperial Valley        | 10/15/1979  | 6.5       | Hartzell and Heaton (1983)  |
| 32         | Imperial Valley        | -           | -         | Archuleta (1984)            |
| 33         | Coyote Lake            | 08/06/1979  | 5.9       | Liu and Helmberger (1983)   |

After performing the spatial slip interpolation, the source-velocity functions (SVFs) are defined on each point of the fault from the functional form employed in the specific inversion study. Stability conditions of the finite-difference calculations implies very short time steps (from 0.005 s to 0.015 s for the larger events). We thus also need to smooth the SVFs to avoid introducing high-frequencies that are not resolved in the inverted source models. This is achieved by convolution with a hamming window of length  $T_{\text{hamm}}=1/F_{\text{max}}$ , where  $F_{\text{max}}$  is the maximum frequency used in the inverted data.

Once the input kinematic models have been interpolated, the fracture energy distributions are obtained from the shear-stress time histories of the dynamic rupture calculations. Average fracture energy is next extracted by calculating its mean value on the slipping area. We define the slipping area as the zone that slipped more than 20% of the mean slip value. This particular choice is motivated by the fact that this area approximately corresponds to the surface region of the raw slip distribution with non-zero slip.

#### 4. SCALING OF FRACTURE ENERGY

To further investigate the scaling of fracture energy, we derive a simple empirical model of the form:  $\log_{10}(W_b) = a \log_{10}(M_0) + b$ , by applying a least-square regression (Figure 4.1). Note that our dataset is composed of 33 source models from 23 earthquakes, with 7 events having more than one published source model. Performing regression using each of the 33 models separately would then require to attribute weights to the individual earthquakes. Therefore, we compute specific empirical models for the 7 multiple-model events, and then derive a single average estimation for the corresponding  $(M_0, W_b)$  couple. Our analysis returns the following relation between breakdown work and seismic moment:

$$\log_{10}(W_b) = 0.59 \log_{10}(M_0) - 10.3 \quad (4.1)$$

This relationship is similar to the one derived by Cocco and Tinti (2008) from a suite of 18 finite-source rupture models from 13 events. Note that we obtain slightly higher values for the coefficients  $a$ , and  $b$ , most likely because Cocco and Tinti (2008) average breakdown work over the entire fault plane, and not only over the slipping area. We also investigate the scaling of  $W_b$  with average slip (Figure 4.1), which leads to:

$$\log_{10}(W_b) = 1.38 \log_{10}(D_m) - 1.2 \quad (4.2)$$

valid for  $D_m$  in the range  $0.05 \leq D_m \leq 4.0$  m. For large events ( $D_m \sim 1$  m) this model is similar to the one derived by Mai et al. (2006) from a much smaller set of spontaneous dynamic rupture calculations that closely match target kinematic inversion models (12 models from 9 events). The model is also compared with the study of Abercrombie and Rice (2005). They obtained:  $\log_{10}(G') = 1.28 \log_{10}(D_m) + 0.72$ , where the quantity  $G'$  is derived from the energy balance between fracture energy, static stress drop and radiated energy. Although their inferred  $G'$  values are smaller than our  $W_b$  estimates (factor  $\sim 2$ ), the overall scaling (i.e, the slope  $a$ ) is very similar, indicating a clear increase with magnitude. The shift (difference in intercept  $b$ ) may arise because Abercrombie and Rice (2005) assume a simple linear slip-weakening model, and thereby neglect possible dynamic undershoot. The quantity  $G'$  may thus underestimate the true fracture energy. Note also that their work is based on smaller magnitude earthquakes, with  $D_m$  from 0.2 mm to 0.2 m.

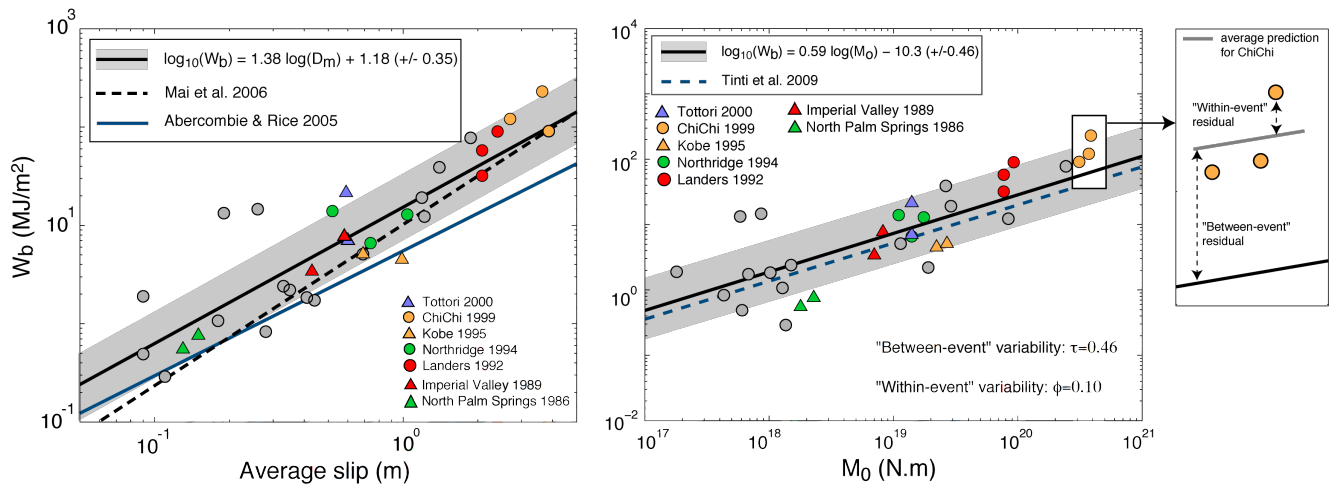


**Figure 4.1.** Empirical model proposed for the average breakdown work  $W_b$  with respect to moment magnitude (top) and mean slip (bottom). The models are compared with the studies of Cocco and Tinti 2008 (blue dashed line), Abercrombie and Rice 2005 (blue solid line) and Mai et al. 2006 (black dashed line). The gray circles

indicate events for which a single model is available; colored symbols indicate rupture for which multiple source inversion results are available.

## 5. UNCERTAINTY ANALYSIS

Although our analysis clearly reveals a scaling of average fracture energy with magnitude, the scatter is rather large. Part of this scatter is epistemic, due to uncertainties in input kinematic inversion models. The robustness of the inferred scaling properties might then be questionable. Epistemic uncertainty can be easily noticed on Figure 4.1, showing that dynamic parameter values for a given event are sensitive to the adopted input kinematic model. This is mainly due to variations in rise-time values and the degree of roughness of the static slip distribution, both of which are inherently difficult to capture by kinematic source inversions.

To test if “poorly resolved” kinematic models may still provide sufficient and robust information to examine the scaling of fracture energy, we perform an uncertainty analysis including the entire set of events for which with several kinematic models are available. The dispersion of the fracture energy values is quantified by splitting the residuals into “between-event” and “within-event” components (Figure 4.1). We thus isolate the “epistemic” variability (due to the uncertainties in the finite-source rupture models) from the “aleatory” variability (arising from the unpredictable randomness of the source process). An equivalent approach is used in empirical ground-motion prediction analyses, to quantify the uncertainties due to various site conditions present for any given ground-motion dataset (e.g. Al-Atik et al. 2010). We therefore compute

(1) the “within-event” variability defined as

$$\phi = \frac{1}{N_m} \sqrt{\sum_{ij} \left( \log_{10}(Wb_{calc. Ei, Mj}) - \log_{10}(Wb_{pred. spec. Ei}) \right)^2} \quad (5.1)$$

where  $N_m$  is the number of rupture models of events studied by several authors ( $N_m = 17$  in our study),  $Wb_{calc. Ei, Mj}$  is the value calculated for model  $M_j$  of event  $E_i$  and  $Wb_{pred. spec. Ei}$  refers to the partial average prediction using only data from event  $E_i$ ;

(2) the “between-event” variability defined as

$$\tau = \frac{1}{N_{evt}} \sqrt{\sum_i \left( \log_{10}(Wb_{pred. spec. Ei}) - \log_{10}(Wb_{pred. glob. Ei}) \right)^2} \quad (5.2)$$

where  $N_{evt}$  is the number of events and  $Wb_{pred. glob. Ei}$  is the global average prediction for event  $E_i$ . The resulting variability (see Figure 4.1) shows that the uncertainties due to several kinematic models for a single event remains small compared to the aleatory variability due the naturally occurring randomness of the rupture process. We therefore claim that the fracture energy scaling revealed by our computations are robust. However, a rigorous analysis of the variability components would require a significantly larger dataset, including multiple models for the whole set of earthquakes; such a dataset is presently not available.

## 6. FAULT STRUCTURAL MATURITY AS A POSSIBLE CONSTRAINT FOR FRACTURE ENERGY ASSESSMENT

Recent studies on stress drop scaling reveal that stress drop values are significantly scattered (*e.g.* Allmann and Shearer, 2009). Based on analyzing data on length ( $L$ ) and maximum slip ( $D_{\max}$ ) for a large suite of earthquakes, Manighetti et al. (2007), conjecture that the apparent variation in stress drop may arise from broken fault segments having variable frictional strength depending on their “structural maturity”. The notion of “structural maturity” is linked to the fault geometry and long-term fault history (age, maximum slip rate, total cumulative displacement), and thus the level of maturity should in principle be predictable for well know active faults. Earthquakes triggering on “immature” faults (that have accumulated little amount of slip) may break only a single segment, and accordingly have large  $D_{\max}/L$  ratio, whereas earthquakes on “mature” faults may more easily propagate onto other segments and thus have lower  $D_{\max}/L$  ratio. Manighetti et al. (2007) propose four different functional forms that well match their  $D_{\max}$ - $L$  measurements from  $\sim 250$  continental earthquakes with various fault mechanisms (see their Figure 2c). The physical model proposed distinguishes two D-L regimes:

$$\begin{aligned} & \text{for ruptures with } L \leq 2W, D_{\max} = \alpha \cdot (L/2) \\ & \text{for ruptures with } L > 2W, D_{\max} = \alpha \cdot 1 / (1/(1/L) + 1/2W) \end{aligned} \quad (6.1)$$

where  $L$  represents the rupture length and  $W$  is the width of the seismogenic layer. The four sets of optimal  $(\alpha, W)$  are listed on figure 6.1.

Through a careful sensitivity analysis (Causse et al, in preparation), we have shown that  $W_b$  is highly sensitive to the spatial distribution of static slip, and particularly to the degree of roughness of slip distributions (*i.e.* their heterogeneity spectrum). To first order, slip roughness may be represented by the ratio  $D_{\max}/L$ . We then use the  $D_{\max}$ - $L$  functions proposed by Manighetti et al. (2007) to partition our set of source models, following the idea that fault maturity could be a strong constraint to refine fracture energy predictions. Two categories are defined: “rough” slip models (best fitted by functions 1-2) and “smooth” slip models (best fitted by functions 3-4) (note that this choice is arbitrary, but our dataset is not large enough to sort the kinematic models according to the 4 proposed functions). Overall, our  $D_{\max}$ - $L$  data are well represented by the set of functions (Figure 6.1). Note that source models associated with the same events have generally similar  $D_{\max}$ - $L$  ratios (or at least fall within the same class, except for the 1992 Landers model). We therefore obtain the following scaling of  $W_b$  with moment magnitude from the two subsets of source models (Figure 6.2):

$$\begin{aligned} & \text{for } D_{\max} / L \geq 5 \cdot 10^{-5}, \quad \log_{10}(W_b) = 0.54 \log_{10}(M_0) - 9.1 \\ & \text{for } D_{\max} / L < 5 \cdot 10^{-5}, \quad \log_{10}(W_b) = 0.62 \log_{10}(M_0) - 11.3 \end{aligned} \quad (6.1)$$

where the value  $5 \cdot 10^{-5}$  is just an approximation to facilitate the distinction between the “rough” and “smooth” slip model classes. This partitioning leads to a significant reduction of the standard deviation, which drops from 0.45 to  $\sim 0.3$ . Again, additional data are needed to better constrain these empirical models. Nevertheless, it shows that fault properties retrieved from geological investigations, such as structural maturity, provide fundamental insights to better predict certain fundamental earthquake source parameters (*i.e.* fracture energy) involved in scaling laws or ground-motion modeling.

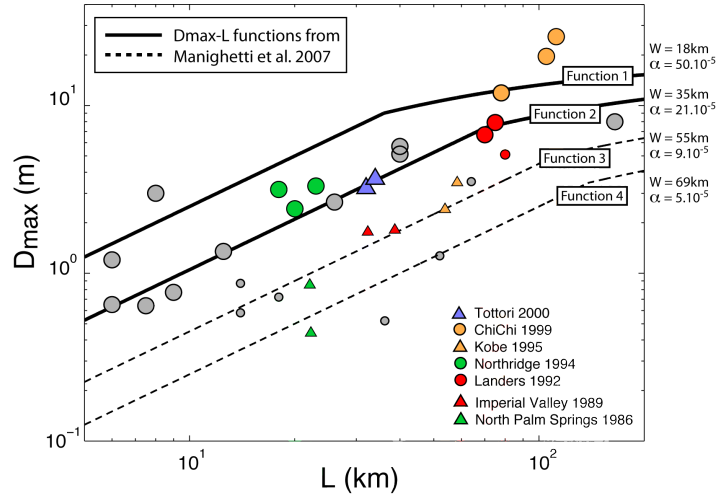


**Figure 6.1.** Distribution of  $D_{\max}$  versus  $L$  for the 33 finite-source rupture models used in this study. We also show the four functional forms proposed by Manighetti et al. (2007). Large markers denote “rough” slip models, better described by functions 1 or 2, whereas small markers are models better represented by functions 3 or 4 (“smooth” slip models).

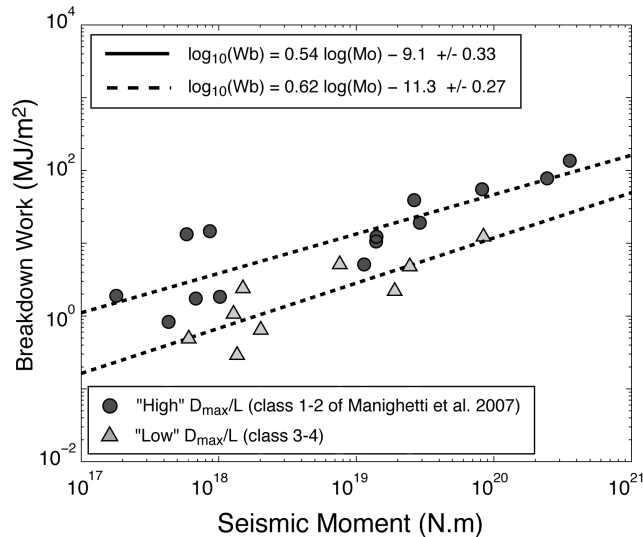


**Figure 6.2.** Empirical models proposed for the average breakdown work  $W_b$ . The  $W_b$  values are split in 2 categories according to their  $D_{\max}/L$  ratio, based on the functional forms proposed by Manighetti et al. (2007). For events having several source models a single  $W_b$  value is shown, so that all the displayed values represent different earthquakes. The standard deviation is significantly reduced (from  $\sim 0.40$  to  $\sim 0.26$ ).

## 7. DISCUSSION AND CONCLUSION

We conduct 3D-dynamic simulations to constrain average fracture energy for 33 kinematic source inversion models from 23 crustal earthquakes. This leads to new empirical models to define average fracture energy with respect to moment magnitude. Our calculations show that fracture energy scales with seismic moment (or mean slip), as reported by previous studies (Abercrombie and Rice 2005, Mai et al. 2006, Cocco and Tinti 2008). The exact physical causes for this scaling are not yet clear. Andrews (1976) demonstrated that for “crack-like” ruptures fracture energy scales as  $\Delta\sigma_s\sqrt{L_h}$ , where  $L_h$  is the distance between the crack tip and the hypocenter. This suggests that rupture expansion during the growth of large earthquakes requires an increasing amount energy to propagate. However, we did not observe any correlation between  $W_b$  and  $L_h$  from our suite of kinematic models, potentially because source inversions tend to return more “pulse-like” models. Campillo et al. (2001) show that

small-scale heterogeneity of fault strength may be represented by effective friction laws. These effective laws lead effective fracture energy all the larger that the heterogeneity characteristic wavelength is large. This suggests that large events potentially have larger scale strength heterogeneities, and accordingly larger fracture energy. This is also suggested by Ohnaka (1999) from lab friction experiments in which larger slip weakening distances were observed for larger geometry irregularities.

The uncertainties in kinematic inversion results strongly affect the robustness of our source parameters estimates. We address this issue through a multiple component variability analysis using the events for which several published source models are available. Our study reveals that only a small fraction of the variability can be attributed to the uncertainties in source inversion. Therefore, we claim that kinematic inversion models still capture the main features for inferring global source dynamic properties.

Since fracture energy is highly sensitive to the roughness degree of slip heterogeneities (Causse et al, in preparation), we develop two empirical models that include the  $D_{\max}/L$  ratio as an additional parameters, based on the  $D_{\max}$ - $L$  functions proposed by Manighetti et al. (2007). This results in a significant decrease of the standard deviation ( $\sigma \approx 0.3$ ). Manighetti et al. (2007) state that  $D_{\max}/L$  is linked to “structural fault maturity”. “Immature” faults are characterized by little accumulated slip, may break only a single fault segment, and accordingly generate earthquakes with large  $D_{\max}/L$  ratio. Earthquakes on “mature” faults may propagate over several fault segments and thus have lower  $D_{\max}/L$ . A simple physical explanation for the potential link between fracture energy and structural maturity, may be that “mature” faults are geometrically smoother, thus may have more homogeneous frictional properties, and accordingly need to spend less energy for the rupture propagation. “Structural maturity”, which is in principle known from geological observation on major faults, could therefore be introduced as a further constraint to refine fracture energy prediction for future earthquakes. The proposed empirical relationships thus provide fundamental input for “pseudo-dynamic” source modelling or spontaneous dynamic rupture simulations. Note that our study only provides the average fracture energy. However the particular spatial distribution can be inferred from *a priori* static slip distributions, assuming proportionality between  $W_b$  and  $D^2$ . Slip distributions can be obtained for instance from spatial random fields or “k-square” like source models (e.g. Mai and Beroza 2002, Causse et al. 2010).

## AKNOWLEDGEMENT

All the numerical computation have been performed on the Shaheen Platform from the KAUST Supercomputing Laboratory.

## REFERENCES

- Abercrombie, R. and J.R. Rice (2005). Can observations of earthquake scaling constrain slip weakening? *Geophys. J. Int.* **162**, 406-424.
- Al Atik, L., N. Abrahamson, J. Bommer, F. Scherbaum, F. Cotton and N. Kuehn (2010). The Variability of Ground-Motion Prediction Models and its Components, *Seismol. Res. Lett.* **81**, 794-801.
- Allmann, B. and P.M. Shearer (2009). Global variations of stress drop for moderate to large earthquakes, *J. Geophys. Res.* **114**, doi :10.1029/2008JB005821.
- Andrews, D. J. (1976). Rupture velocity of plane strain shear cracks, *J. Geophys. Res.* **81**, 5679-5687.
- Bizzarri, A. (2010). On the relations between fracture energy and physical observables in dynamic earthquake models, *J. Geophys. Res.* **115**, B10307, doi:10.1029/2009JB007027.
- Burjanek, J. and J. Zahradnik (2007). Dynamic stress field of a kinematic earthquake source model with k-squared slip distribution, *Geophys. J. Int.*, doi: 10.1111/j.1365-246X.2007.03548.x.

- Campillo, M., P. Favreau, I.R. Ionescu and C. Voisin (2001). On the effective friction law of a heterogeneous fault, *J. Geophys. Res.* **106**, 16307-16322.
- Causse, M., E. Chaljub, F. Cotton, C. Cornou and P.Y. Bard (2009). New approach for coupling  $k^2$  and empirical Green's functions: Application to the blind prediction of broadband ground-motion in the Grenoble basin, *Geophys. J. Int.* **179**, 1627-1644.
- Causse, M., F. Cotton and P.M. Mai (2010). Constraining the roughness degree of slip heterogeneity, *J. Geophys. Res.* **115**, B05304, doi:10.1029/2009JB006747.
- Cocco, M. and E. Tinti (2008). Scale dependence in the dynamics of earthquake propagation: evidence from seismological and geological observations, *Earth planet. Sci. Lett.* **273**, 123-131.
- Dalguer, L. A. and S.M. Day (2007). Staggered-Grid Split-Node Method for Spontaneous Rupture Simulation. *J. Geophys. Res.*, **112**, B02302, doi:10.1029/2006JB004467 .
- Fukuyama, E., T. Mikumo and K.B. Olsen (2003). Estimation of the critical slip-weakening distance: theoretical background, *Bull. seism. Soc. Am.* **93**, 1835-1840.
- Guatteri, M., P.M. Mai, and G.C. Beroza (2004). A pseudo-dynamic approximation to dynamic rupture models for strong ground motion prediction, *Bull. Seismol. Soc. Am.*, **94**, 2051-2063.
- Kanamori, H. and L. Rivera (2004). Static and dynamic scaling relations for earthquakes and their implications for rupture speed and stress drop, *Bull. Seismol. Soc. Am.* **94**, 314-319.
- Mai, P.M., P. Somerville, A. Pitarka, L. Dalguer, S. Song, G. Beroza, H. Miyake and K. Irikura (2006). On scaling of fracture energy and stress drop in dynamic rupture models: consequences for near-source groundmotions, in *Earthquakes Radiated Energy and the Physics of Faulting* **170**, pp. 283-293, eds Abercrombie, R., McGarr, A., Kanamori, H. & Di Toro, G., Geophysical Monograph Series, American Geophysical Union, doi:10.1029/170GM28.
- Mai, P. M. and G. C. Beroza (2002). A spatial random field model to characterize complexity in earthquake fields, *J. Geophys. Res.* **107**(B11), 2308, doi:10.1029/2001JB000588.
- Mai, P.M., J. Burjanek, B. Delouis, G. Festa, C. Francois-Holden, D. Monelli, T. Uchide, J. Zahradnik. Source-inversion blindtest: initial results and further developments (2007). *Eos Trans. AGU*, 88(52), Fall Meet. Suppl., Abstract S53C-08.
- Manighetti, I., M. Campillo, S. Bouley and F. Cotton (2007). Earthquake scaling, fault segmentation and structural maturity, *Earth and Planetary Science Letters* **253**, 429-438.
- Mikumo, T., K. B. Olsen, E. Fukuyama, and Y. Yagi (2003). Stress-breakdown time and slip-weakening distance inferred from slip velocity functions on earthquake faults, *Bull. Seismol. Soc. Am.* **93**, 264 - 282.
- Ohnaka, M. and L. Shen (1999). Scaling of the share rupture process from nucleation to dynamic propagation: Implication of geometry irregularity of the rupturing surfaces, *J. Geophys. Res.* **104**, 817-844.
- Piatanesi, A., E. Tinti, M. Cocco and E. Fukuyama (2004). The dependence of traction evolution on the earthquake source time function adopted in kinematic rupture models, *Geophys. Res. Lett.* **31**, doi:10.1029/2003GL019225.
- Rice, J. R., C. G. Sammis and R. Parson (2005). Off-fault secondary failure induced by a dynamic slip pulse, *Bull. Seismol. Soc. Am.* **95**, 109-134.
- Spudich, P., and M. Guatteri (2004). The effect of bandwidth limitations on the inference of earthquake slip-weakening distance from seismograms, *Bull. Seismol. Soc. Am.* **94**, 2028-2036.
- Tinti, E., P. Spudich and M. Cocco (2005a). Earthquake fracture energy inferred from kinematic rupture models on extended faults, *J. geophys. Res.* **110**, doi:10.1029/2005JB00364.
- Tinti, E., P. Spudich and M. Cocco (2008). Correction to « Earthquake fracture energy inferred from kinematic rupture models on extended faults », *J. geophys. Res.* **113**, B07301, doi:10.1029/2008JB005829.
- Tinti, E., E. Fukuyama, A. Piatanesi and M. Cocco (2005b). A kinematic source time function compatible with earthquake dynamics, *Bull. seism. Soc. Am.* **95**, 1211-1223.
- Tinti, E., M. Cocco, E. Fukuyama and A. Piatanesi (2009). Dependence of slip weakening distance ( $D_c$ ) on final slip during dynamic rupture of earthquakes, *Geophys. J. Int.* **177**, 1205-1220.
- Wald, D. J. (1996). Slip history of the 1995 Kobe, Japan, earthquake determined from strong motion, teleseismic, and geodetic data. *J. Phys. Earth* **44**, 489-503.
- Yoshida, S., K. Koketsu, B. Shibasaki, T. Sagiya, T. Kato, and Y. Yoshida. (1996). Joint inversion of near- and far-field waveforms and geodetic data for the rupture process of the 1995 Kobe earthquake. *J. Phys. Earth* **44**, 437-454.